



RESEARCH ARTICLE

Clinical utility of intraoperative arterial spin labeling for resection control in brain tumor surgery at 3 T

Marta Calvo-Imirizaldu¹  | Verónica Aramendía-Vidaurreta^{1,2} |
 Carmen Sánchez-Albardíaz¹ | Marta Vidorreta³ | Reyes García de Eulate¹ |
 Pablo D. Domínguez Echávarri^{1,2} | Josef Pfeuffer⁴ | Bartolomé Bejarano Herruzo⁵ |
 Lain H. Gonzalez-Quarante⁵ | Antonio Martinez-Simon⁶ | María A. Fernández-Seara^{1,2} 

¹Radiology Department, Clínica Universidad de Navarra, Pamplona, Spain

²IdiSNA, Instituto de Investigación Sanitaria de Navarra, Pamplona, Spain

³Siemens Healthcare, Madrid, Spain

⁴Application Development, Siemens Healthcare, Erlangen, Germany

⁵Neurosurgery Department, Clínica Universidad de Navarra, Pamplona, Spain

⁶Anesthesia and Intensive Care Department, Clínica Universidad de Navarra, Pamplona, Spain

Correspondence

María A. Fernández Seara, Radiology, Clínica Universidad de Navarra, Avenida Pio XII 36, 31008 Pamplona, Navarra, Spain.
 Email: mfseara@unav.es

Funding information

Ph.D. grant support from Siemens Healthcare Spain (M.C.I.); Spanish Ministry of Science and Innovation, Instituto de Salud Carlos III, AES Program grant, Grant/Award Number: PI18/00084 (M.F.S.)

Resection control in brain tumor surgery can be achieved in real time with intraoperative MRI (iMRI). Arterial spin labeling (ASL), a technique that measures cerebral blood flow (CBF) non-invasively without the use of intravenous contrast agents, can be performed intraoperatively, providing morpho-physiological information. This study aimed to evaluate the feasibility, image quality and potential to depict residual tumor of a pseudo-continuous ASL (PCASL) sequence at 3 T. Seventeen patients with brain tumors, primary (16) or metastatic (1), undergoing resection surgery with iMRI monitoring, were prospectively recruited (nine men, age 56 ± 16.6 years). A PCASL sequence with long labeling duration (3000 ms) and post-labeling delay (2000 ms) was added to the conventional protocol, which consisted of pre- and postcontrast 3D T_1 -weighted (T_1w) images, optional 3D-FLAIR, and diffusion. Three observers independently assessed the image quality (four-point scale) of PCASL-derived CBF maps. In those with diagnostic quality (Scores 2–4) they evaluated the presence of residual tumor using the conventional sequences first, and the CBF maps afterwards (three-point scale). Inter-observer agreement for image quality and the presence of residual tumor was assessed using Fleiss kappa statistics. The intraoperative CBF ratio of the surgical margins (i.e., perilesional CBF values normalized to contralateral gray matter CBF) was compared with preoperative CBF ratio within the tumor (Wilcoxon's test). Diagnostic ASL image quality was observed in

Abbreviations: 3D-TOF, 3D time of flight; ASL, arterial spin labeling; ATT, arterial transit time; CBF, cerebral blood flow; DSC, dynamic susceptibility contrast enhanced; FLAIR, fluid attenuated inversion recovery; GRASE, 3D gradient and spin echo; iMRI, intraoperative MRI; LT, labeling time; PCASL, pseudo-continuous ASL; PLD, postlabeling delay; ROI, region of interest; SNR, signal-to-noise ratio; WHO, World Health Organization; κ , kappa.

This is an open access article under the terms of the [Creative Commons Attribution-NonCommercial-NoDerivs](https://creativecommons.org/licenses/by-nc-nd/4.0/) License, which permits use and distribution in any medium, provided the original work is properly cited, the use is non-commercial and no modifications or adaptations are made.

© 2023 The Authors. *NMR in Biomedicine* published by John Wiley & Sons Ltd.

94.1% of patients (interobserver Fleiss $\kappa = 0.76$). PCASL showed additional foci suggestive of high-grade residual component in three patients, and a hyperperfused area extending outside the enhancing component in one patient. Interobserver agreement was almost perfect in the evaluation of residual tumor with the conventional sequences (Fleiss $\kappa = 0.92$) and substantial for PCASL (Fleiss $\kappa = 0.80$). No significant differences were found between pre and intraoperative CBF ratios ($p = 0.578$) in patients with residual tumor ($n = 7$). iMRI-PCASL perfusion is feasible at 3 T and is useful for the intraoperative assessment of residual tumor, providing in some cases additional information to the conventional sequences.

KEYWORDS

arterial spin labeling, brain tumor, intraoperative MRI, neuro-oncology, perfusion imaging, residual neoplasm

1 | INTRODUCTION

Gliomas are the most common primary malignant tumors of the brain, among which glioblastoma is the most frequent and malignant histologic type, classified as Grade 4 in the WHO (World Health Organization) classification.^{1,2} The brain is also a frequent site for metastasis of non-central nervous system tumors, most frequently from lung, breast and melanoma.³ Therapeutic options are limited. Surgical resection is the treatment of choice in high-grade tumors, when the location of the tumor does not carry a risk of causing functional deficits. In these tumors, surgery is followed by adjuvant radiochemotherapy (Stupp protocol)⁴ to achieve the maximal safe cytoreduction, which has been proven to lead to longer survival times and better quality of life.^{5–11} Complete macroscopic resection is defined as “gross total resection,” characterized by the absence of contrast enhancement after surgery.⁵ While there may also be non-enhancing residual tumor, some studies demonstrated an inverse correlation between the postoperative enhancement volume and survival in high grade tumors.^{12,13} Nevertheless, recent studies also support the association between the postoperative residual non-enhancing volume and a worst prognosis.¹⁴

Developments in imaging techniques now allow the evaluation of the extent of resection in real time with intraoperative MRI (iMRI), providing accurate and immediate information while minimizing the rates of reintervention and risk of damage of eloquent regions.^{15–18} Its use has been correlated with improved neurological outcomes and longer survival times.¹⁹ On the other hand, the main disadvantage of using iMRI is its high cost and the increase of the procedure duration.²⁰

Currently, available iMRI units at 1.5 T and 3 T allow the implementation of advanced imaging protocols including diffusion and perfusion.²¹ Cerebral perfusion can be assessed using dynamic susceptibility contrast (DSC), a technique that has been evaluated intraoperatively, with promising results.^{22,23} These previous studies showed that DSC perfusion was useful to confirm total resection and evinced residual tumor in cases of incomplete resection even more reliably than postcontrast T1w images alone, suggesting that it could be used as a complementary tool for resection control. However, DSC requires the administration of an intravenous contrast agent, which limits its repeatability. Arterial spin labeling (ASL) is a novel MRI technique that measures cerebral blood flow (CBF) non-invasively without the use of contrast media.²⁴ In ASL, blood water is magnetically labeled and the effects of this label in the tissue are measured after a delay time, by comparison with a control condition. If the delay time is sufficiently long for the water spins to reach the capillary bed or tissue, ASL signal is directly proportional to CBF, and absolute CBF measurements can be calculated. Studies have shown the role of ASL in neuro-oncology for the diagnosis, grading and therapy monitoring of gliomas, with results comparable to those of conventional DSC.^{25–29} However, the potential of ASL to assist in the intraoperative setting has been scarcely explored. Two studies including small patient cohorts and performed at the same site have been reported, with results suggesting that intraoperative ASL is feasible at 1.5 T and could provide useful information for resection control.^{30,31} However, the technique has not been evaluated at higher field (3 T), which could in principle provide higher SNR through the combination of higher field and longer T_1 , but where issues related to magnetic field inhomogeneities are exacerbated and could reduce the labeling efficiency, in turn decreasing the signal-to-noise ratio (SNR) and compromising image quality. Moreover, iMRI is performed under anesthesia, generally achieved by intravenous infusion of propofol and remifentanyl, while a state of normocapnia is maintained by mechanical ventilation. In these conditions CBF is expected to decrease with respect to normal values in non-anesthesia conditions,^{32,33} while arterial transit time (ATT) is expected to increase.³⁴ These changes must be considered when selecting the pseudo-continuous ASL (PCASL) parameters.

Thus, the purpose of this study was to evaluate the feasibility of performing ASL in the iMRI setting at 3 T, and to assess image quality and potential to depict residual tumor. To this end, a PCASL sequence was tested in patients with brain tumors, using long labeling to improve the SNR. We hypothesized that the use of ASL would lead to a higher rate of residual tumor depiction than using conventional sequences alone.

2 | METHODS

2.1 | Patient selection

The study was approved by the local ethics committee. Between December 2020 and March 2022, 37 patients were identified as having brain tumors, primary or metastatic, requiring surgery. Only patients undergoing iMRI for resection control were included in the study. Exclusion criteria were the presence of cardiopulmonary or hepatorenal comorbidities, contraindications to MRI and inability to give consent. Finally, a total of 17 patients were eligible for the study. Informed consent was obtained from all patients.

2.2 | iMRI protocol

The iMRI examinations were performed on a 3 T MRI scanner (MAGNETOM Skyra, Siemens, Erlangen, Germany) using two four-channel flexible coils (Flex Small 4 and Flex Large 4, Siemens, Erlangen, Germany) for reception. This equipment is located within the surgical area with direct access to the operating room.

The clinical conventional protocol included precontrast 3D-T1w images (MPRAGE—magnetization prepared rapid acquisition gradient echo), diffusion, optional 3D-T₂ FLAIR (fluid attenuated inversion recovery) (in patients with low-grade tumors with no enhancing component) and post-contrast 3D-T1w images. For this study, a prototype 3D-PCASL sequence³⁵ with a 3D gradient and spin echo (GRASE) readout with background suppression, long labeling duration (LD = 3000 ms) and postlabeling delay (PLD = 2000 ms) was added to the protocol before contrast injection. The sequence allowed independent planning of the imaging volume and the labeling plane, which was positioned perpendicular to the carotid and vertebral arteries, based on an angiogram previously acquired using a 3D time of flight (3D-TOF) sequence. PCASL acquisition parameters are detailed in Table 1.

All patients had been previously subjected to preoperative MRI in the same scanner for neuronavigation planning that included a preoperative PCASL sequence in 14 out of the 17 patients. Preoperative PCASL parameters are included in Data S1 Section 5 (Supplementary Table 1).

2.3 | Intraoperative setting

Before surgery, patients were placed in an MRI-compatible head frame (DORO LUCENT iMRI Headrest System, Freiburg, Germany) with MRI-compatible titanium pins, positioned according to the surgical demands in either prone, supine, or lateral position. The transfer to the MRI suite took place during the intervention, when the neurosurgeon judged the resection to be complete or maximally safe.

During iMRI all patients except one received general anesthetics (target control infusion of propofol 2.8–3.5 µg/mL and remifentanyl 0.5–2 ng/mL). The remaining patient underwent awake craniotomy with cooperative sedation for exploration of eloquent areas, where dexmedetomidine 0.4–0.8 µg/kg/h and remifentanyl 0.5–2 ng/mL were employed. At the moment of the iMRI the patient was under deep sedation.

TABLE 1 PCASL 3D-GRASE sequence parameters.

Readout sequence	3D GRASE
T _R /T _E (ms)	6500/20.5
EPI/TSE factor/number of segments	31/16/2
In-plane voxel size (mm ²)	4.0 × 4.0
Parallel imaging	GRAPPA 2
Slice thickness (mm)/number of slices/SliceOS	5/26/17.5%
Field of view (mm ²)	256 × 256
Number of background suppression pulses	4
Labeling duration/PLD (ms)	3000/2000
Number of label and control pairs	12
Total time (including an M0 scan)	5 min 30 s

T_R, repetition time; T_E, echo time; EPI, echo-planar imaging; TSE, turbo spin echo; OS, oversampling; M0, proton density image; GRASE, gradient and spin echo.

The primary objective of the iMRI study was to determine the extent of resection, assessed by a neuroradiologist in collaboration with the neurosurgeon. Resection was considered complete, incomplete, or uncertain based on conventional sequences. In contrast-enhancing tumors the resection was defined as complete when no residual increased signal intensity on contrast-enhanced T1w images was assessed near the surgical margins, or when only a thin linear enhancement attributable to inflammatory reparative changes was seen. Incomplete or uncertain resection was defined as gross, non-linear, contrast enhancement. In non-enhancing tumors, residual tumor was assessed using T_2 fluid-attenuated inversion recovery (FLAIR), as the area of increased signal intensity corresponding to the defined mass lesion, or non-enhancing tumoral hypointensity on T1w images.⁵ If iMRI revealed residual tumor that could be resected without damaging important structures, the surgery continued after the scan. Otherwise, if resection was considered complete, the neurosurgeon proceeded to finish the intervention. PCASL data were not considered in the clinical decision-making process.

Postoperative MRI evaluation was performed within 24–72 h to confirm the extent of resection, using the clinical conventional protocol only. Neoplastic grading was assigned by histopathology according to the WHO classification updated in 2021.²

The configuration of receiver coils, stereotactic frame and fixation screws employed in the iMRI was evaluated in three healthy volunteers outside the surgical setting. For detailed methods and results see Data S1 Section 4.

2.4 | Postprocessing

CBF maps were calculated at the scanner after subtraction of labeled and control images, according to Buxton's model³⁶ and equations from Alsop et al.²⁴

Images were transferred to a workstation equipped with commercially available postprocessing software (syngo.via VB30A, Siemens Healthcare), MRIcron (Neuroimaging Tools and Resources Collaboratory) and MATLAB (2020) (Version 9.9.0 (R2020b), MathWorks, Natick, MA, USA).

2.5 | Image quality of PCASL images

For the purpose of the study, visual quality control was conducted for the detection of clinically usable and non-usable CBF maps by three neuro-radiologists (PDE, RGE and MCI, with 2, 7 and 2 years of experience evaluating ASL data, respectively) independently. A four-point Likert scale was used, following previous published examples by Ferro et al.,³⁷ considering Score 4, good quality (maps with good tissue perfusion and without vascular contrast), Score 3, acceptable (minor vascular contrast and reasonable tissue perfusion), Score 2, angiogram (predominantly vascular contrast, low tissue perfusion) and Score 1, uninterpretable (very low signal, likely due to labeling error or severe susceptibility artifacts). The results were discussed a posteriori, and in cases of disagreement a consensus was reached. Scores 2–4 were considered of diagnostic quality.

2.6 | Resection control

Datasets of diagnostic quality were evaluated by the same observers to assess the presence of residual tumor. Two scores were obtained, the first one with information on the conventional sequences alone, and the second one according to the PCASL perfusion maps overlaid on the post-contrast T_1 (which was needed for proper evaluation of CBF near the surgical margins, in order to exclude confounders such as vascular structures), using a three-point rating scale as described in Table 2. In cases of disagreement, a consensus was reached a posteriori.

TABLE 2 Three-point rating scale criteria to evaluate the presence of residual tumor in conventional sequences and PCASL.

Score	Conventional sequences	PCASL
0	No visible increased signal intensity on contrast-enhanced T1w MR images near the surgical margins, or only a thin linear enhancement attributable to inflammatory reparative changes	No visible areas of high CBF
1	Gross, non-linear, contrast enhancement on T1w, or non-enhancing hypointensity on T1w or hyperintensity on FLAIR, suggestive of low-grade component	Presence of a clearly defined area of elevated CBF surrounding the surgical cavity (not corresponding to a vascular structure)
X	Unclear lesion	Unclear lesion

2.7 | CBF ratio calculation

Measurements of perilesional CBF were performed in the preoperative PCASL scan (if available) and in the intraoperative scan for each patient.

Even though ASL provides absolute CBF values, we computed normalized CBF using the contralateral gray matter CBF value as reference, to avoid possible intraindividual changes in CBF due to anesthetic conditions in the comparison of preoperative and intraoperative data.

If a presumed residual enhancing lesion was present, a circular region of interest (ROI), of approximately 0.4–0.6 cm², was manually positioned in a single slice, over the highest CBF area within the region of suspected residual tumor, avoiding the regions of vessels, hemorrhage and necrosis, using the platform MRICron. When no residual enhancing tumor was visible, the ROI was positioned in the non-enhancing component (if present), or in the border of the surgical cavity, according to the neuroradiologist criteria. Gray matter masks were obtained by segmenting the precontrast T1w anatomical images with MATLAB using SPM12. Once the segmentation was obtained an intensity filter with a threshold of 0.9 was applied, generating binary masks. Then the contralateral gray matter was selected only for the slice where the tumor ROI was positioned. Mean CBF values of this mask were obtained (MRICron). An example can be found in Figure 1.

Finally, the maximum value of tumor ROI was divided by the mean value of contralateral normal gray matter ROI to estimate CBF ratios.^{29,38,39}

We did not have preoperative PCASL data for Patients 6, 7 and 11.

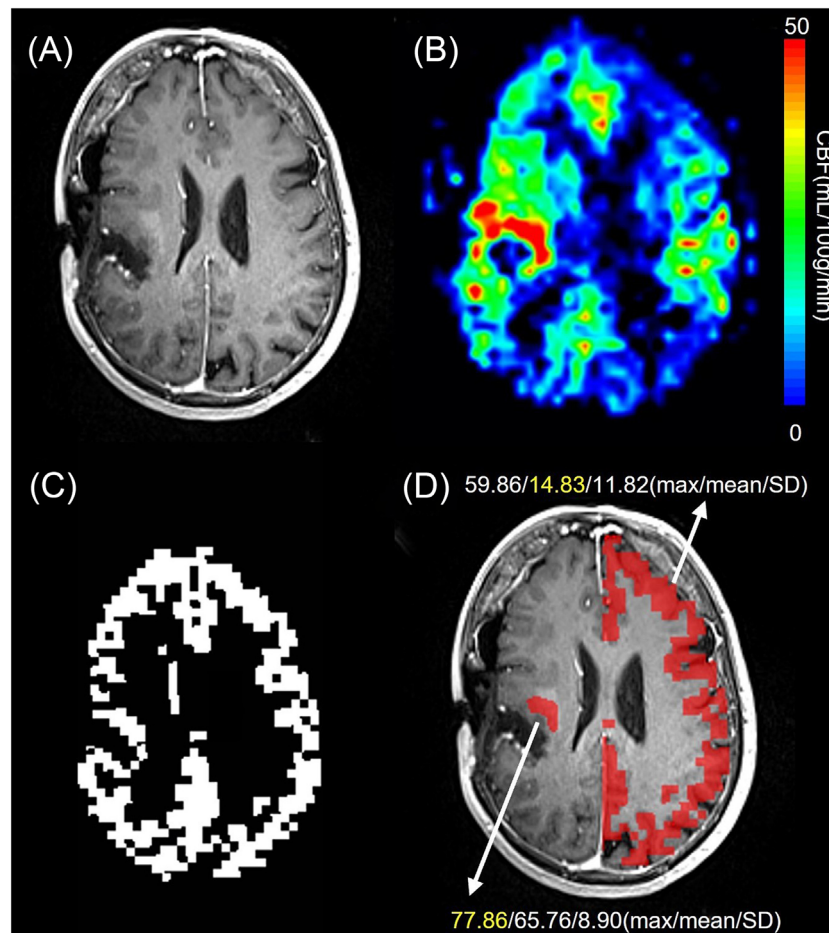


FIGURE 1 Measurements of CBF ratios. Example in an 81-year-old woman with a right frontotemporal oligodendroglioma IDH mutant and 1p/19q co-deleted, Grade 3 (additional images from this patient are included in Figure 5). (A), Intraoperative postcontrast T1w image showed faint enhancing residual component in the medial aspect of the surgical cavity. (B), The CBF map from the intraoperative PCASL sequence at the same slice showed high CBF in the residual lesion. The ROI was manually positioned in the highest CBF area within the region of suspected residual tumor, avoiding the regions of vessels, hemorrhage and necrosis, as shown in D. (C), A gray matter mask was segmented from precontrast T1w images with SPM12; the gray matter mask is shown at the slice of the tumor. (D), Representation of the tumor ROI and contralateral gray matter mask over the anatomical T1w image, with the CBF values obtained (expressed in units of mL/100 g/min). The CBF ratio was calculated by dividing the maximum value of tumor ROI by the mean value of contralateral normal gray matter ROI; in this case, CBF ratio = $77.86/14.83 = 5.25$.

2.8 | Statistical analysis

Interobserver agreement for image quality and residual tumor was assessed with kappa statistics (κ), using the Fleiss kappa correlation coefficient for three raters (R package “stats,” Version 2.15.3). For image quality three categories were considered: scores 4 + 3, score 2 and score 1. κ values were interpreted according to the criteria of Landis and Koch⁴⁰ for agreement: <0, poor; 0.10–0.20, slight; 0.21–0.40, fair; 0.41–0.60, moderate; 0.61–0.80, substantial; 0.81–1.00, almost perfect.

Wilcoxon's test was performed to test differences in intraoperative CBF ratio and that of the preoperative tumor, for each patient. Two subgroups were analyzed separately, one including patients with suspected residual tumor, and the other including patients with complete radiological resection, according to the conventional sequences.

A chi-square test was performed to evaluate the association between the results of residual tumor detection performed with conventional sequences and PCASL (IBM SPSS Statistics Version 22.0). $p \leq 0.05$ was considered statistically significant.

3 | RESULTS

3.1 | Patients

17 patients met the inclusion criteria (9 men, mean age 56 ± 16.6 years). 15 patients had high-grade primary brain tumors, one patient had low-grade astrocytoma and one patient had brain metastasis from lung carcinoma. Patient characteristics and tumor histopathological details are detailed in Table 3.

3.2 | Quality assessment of PCASL images

Interobserver agreement for image quality was substantial (Fleiss $\kappa = 0.76$).

According to the consensus score reached a posteriori, diagnostic image quality was observed in 94.1% of the patients (16/17). Image quality was good (Score 4) in 9/17 maps (53%) and acceptable (Score 3) in 4/17 maps (24%). An angiogram-like rating (Score 2) was determined in 3/17 maps (18%) and uninterpretable (Score 1) was found in 1/17 map (5%) (see Table 4). Figure 2 shows examples of good, acceptable, angiogram-like and uninterpretable CBF maps. Acquired imaging data on the three patients with angiogram-like PCASL images (Nos. 1, 5 and 12 in Table 4) are presented in Data S1 Section 1. The patient with uninterpretable image quality (no 17) was excluded from subsequent analysis. Available data on this patient are included in Data S1 Section 2.

3.3 | Resection control

According to the consensus evaluation, the assessment with conventional sequences determined complete resection in seven patients, where PCASL also determined complete removal (Nos. 3, 5, 7, 8, 9, 13 and 15). Ten patients had residual tumor according to the conventional sequences, including the patient with low-quality PCASL data (No. 17, who was not included in the analysis). In 5 of these 10 patients the surgery continued based on the information provided by iMRI. In the other 5 patients it was not possible to continue the resection, as it carried risk of damaging eloquent areas due to the location of the residual tumor.

Of the nine patients included in the analysis that showed residual component in the conventional sequences, six presented enhancing component (Nos. 2, 10, 11, 12, 14 and 16) and three had a non-enhancing lesion (Nos. 1, 4 and 6). PCASL maps displayed residual hyperperfused component in five of the six patients with enhancing component (Nos. 2, 10, 11, 12, 14). In one of these patients PCASL revealed additional hyperperfused suspicious components located far from the contrast enhancement (No. 2), and in another patient PCASL showed very high CBF that appeared to extend outside the enhancing component (No. 10) (Table 4). In Patient 16, residual tumor with contrast enhancement was observed in the conventional sequences; however, no hyperperfusion was found in PCASL CBF maps.

In two of the three patients judged to have non-enhancing residual tumor based on conventional imaging, PCASL showed a hyperperfused focal lesion within the non-enhancing tissue (Nos. 1 and 6). In the remaining patient (No. 4), no hyperperfusion was observed.

The four cases in which PCASL provided information that was not present in the conventional sequences are presented. Figure 3 shows a patient presenting a nodular contrast enhancing component (No. 2) that had an additional spot of high CBF on the PCASL maps relatively remote from the enhancing mass, suggestive of another residual tumoral component that was not depicted in T1w postcontrast images. Follow-up revealed likely residual tumor as supported by subsequent tumor growth in this region. Another patient (No. 1, Figure 4) had non-enhancing residual tumor, but showed an area of high CBF on PCASL maps within this lesion. 11C-methionine-PET performed one month postsurgery revealed

TABLE 3 Patient demographic and clinical characteristics.

Characteristic	Value	
Number of patients		
Total	17	
Men	9	
Women	8	
Age (yr: mean (range; SD))	56 (11–81; 16.7)	
First surgery (%)	94	
WHO grade ^a		
1	0	
2	1	
3	4	
4	11	
Metastasis	1	
Histological entities	Primarily enhancing	Primarily non-enhancing
Glioblastoma WHO Grade 4	11	
Astrocytoma WHO Grade 3	3	
Oligodendroglioma WHO Grade 3	1	
Astrocytoma WHO Grade 2		1
Lung metastasis	1	

^aApplied to primary (glial) tumors (fifth edition of the WHO Classification of Tumors of the Central Nervous System²).

increased metabolic activity in the same location, supporting the presence of residual tumor. Patient No. 10 (Figure 5) had a highly vascularized right frontotemporal lesion in the preoperative MRI evaluation that could not be completely resected due to close proximity to white matter tracts. The iMRI showed markedly high CBF on PCASL maps surrounding the anterior and medial border of the surgical cavity that extended beyond the enhancing lesion depicted by the conventional sequences. Patient No. 6 had a diffuse astrocytoma Grade 2, which showed high areas of CBF values within the non-enhancing component on PCASL maps compared with the contralateral side. Surgery was not continued in this case, because of the location of the lesion (Wernicke's area) and considering that the tumor was low grade without fluorescent signal.

Finally, in Patient No. 4 non-enhancing residual tumor was found with the conventional sequences, without visible elevation of CBF values on PCASL maps.

3.4 | Interobserver agreement for resection control

Interobserver agreement among the three readers was almost perfect in the evaluation of the conventional sequences (Fleiss $\kappa = 0.92$), and substantial in the depiction of residual tumor with the PCASL maps (Fleiss $\kappa = 0.80$).

3.5 | CBF ratio

Patients 6, 7 and 11 were not eligible for this evaluation. Considering this, intraoperative CBF ratios were compared with preoperative CBF ratios of the homologous region in two subgroups: patients with residual tumor ($n = 7$) and patients with complete resection ($n = 6$) (Table 4).

In the total sample, preoperative CBF ratios varied from 1.43 to 6.75, while intraoperative CBF ratios varied from 0.32 to 5.25.

The analysis in the subgroup of patients with residual tumor found no significant differences ($p = 0.578$) between the preoperative tumoral CBF ratios and intraoperative CBF ratios in the presumed residual tumor.

On the other hand, significant differences existed between preoperative and intraoperative CBF ratios in those patients with complete tumor removal ($p = 0.031$).

TABLE 4 Consensus evaluation of resection control assessed with the conventional protocol and with the PCASL sequence, correlated to normalized CBF ratios obtained from preoperative and intraoperative PCASL data.

Patient (No./sex/age)	Histologic diagnosis and WHO grade	Image quality (consensus)	Resection control by conventional protocol	Resection control by PCASL	Preoperative CBF ratio	Intraoperative CBF ratio
1/M/47	Astrocytoma WHO Grade 3	2	1 (no enhancement)	1 ^a	1.98	2.9
2/M/52	Glioblastoma WHO Grade 4	4	1	1 ^b	2.94	4.77
3/F/52	Astrocytoma WHO Grade 3	4	0	0	2.53	1.28
4/M/51	Glioblastoma WHO Grade 4	3	1 (no enhancement)	0	1.73	0.95
5/M/54	Astrocytoma WHO Grade 3	2	0	0	2.46	0.97
6/M/76	Astrocytoma WHO Grade 2	4	1 (no enhancement)	1 ^a	NA	1.09
7/F/59	Glioblastoma WHO Grade 4	4	0	0	NA	0.41
8/M/11	Glioblastoma WHO Grade 4	4	0	0	1.43	0.83
9/F/38	Glioblastoma WHO Grade 4	4	0	0	1.51	0.32
10/F/81	Oligodendroglioma WHO Grade 3	3	1	1 ^c	6.75	5.25
11/F/45	Glioblastoma WHO Grade 4	4	1	1	NA	1.21
12/M/70	Glioblastoma WHO Grade 4	2	1	1	6.46	1.27
13/F/63	Glioblastoma WHO Grade 4	4	0	0	2.44	1.08
14/M/72	Glioblastoma WHO Grade 4	3	1	1	3.45	2.70
15/F/53	Glioblastoma WHO Grade 4	4	0	0	2.83	0.51
16/F/48	Lung metastasis	3	1	0	1.87	1.50
17/M/70 (excluded)	Glioblastoma WHO Grade 4	1	1	NA	2.48	NA
Mean ± SD					2.51 ± 1.40	1.69 ± 1.48

M, male; F, female; 0, complete resection; 1, tumor remaining; 1^a, hyperperfused residual lesion identified with PCASL within non-enhancing lesion; 1^b, additional residual lesion identified with PCASL only; 1^c, very high-CBF area extending outside the enhancing component. NA, not available.

3.6 | Association between conventional sequences and PCASL

The chi-square test determined a significant relationship between the evaluation of residual tumor using conventional sequences and PCASL ($p = 0.001$).

4 | DISCUSSION

Our study proves the feasibility of obtaining PCASL data intraoperatively in a 3 T scanner using flexible coils. We used a 3D-GRASE PCASL sequence that offered greater immunity against susceptibility artifacts and better SNR than the previously employed EPI sequence. Moreover, data were acquired using a single PLD and long labeling time (LT). The long LT was chosen to increase the SNR, as the ASL signal increases with label duration.^{24,41} It also had the effect of increasing the delay time for the spins that were labeled earlier, resulting in more sensitivity for perfusion with a longer transit time and contributing to reduced artifacts from long arrival times.⁴²

In terms of image quality, we obtained diagnostic image quality in 94.1% of the patients, while in one patient the PCASL data were uninterpretable. This was likely due to ineffective labeling caused by off-resonance effects at the labeling plane. However, the data obtained during the examination did not provide any conclusive proof, because B_0 maps were not acquired at the labeling plane. The TOF angiogram was of good quality; however, the TOF magnitude images showed some artifacts that could also be due to off-resonance frequencies (see Data S1 Section 2). The tumor in this patient was located in the right temporo-occipital lobe so the surgical cavity was closer to the labeling plane than in other cases, and the presence of air in the cavity could have exacerbated the off-resonance effects.

Even though the majority of patients had good and acceptable scores, three studies were rated as angiogram like, which could possibly be explained by long ATT. In older patients or in patients under general anesthesia, blood velocity might be reduced (see Data S1 Section 3), leading to long ATT, thus causing labeled blood to remain inside the major intracranial arteries at the time of readout, without reaching the capillary bed, and generating images with low parenchymal perfusion potentially leading to misinterpretation.^{31,43} In this study, we used the

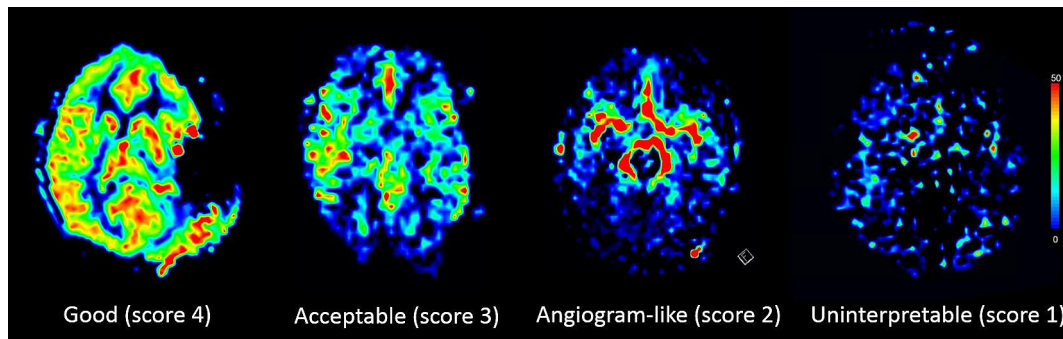


FIGURE 2 Rating of PCASL image quality, with example representations for good, acceptable, angiogram-like and uninterpretable image quality scores of CBF maps. The figure demonstrates the different image qualities observed in our sample.

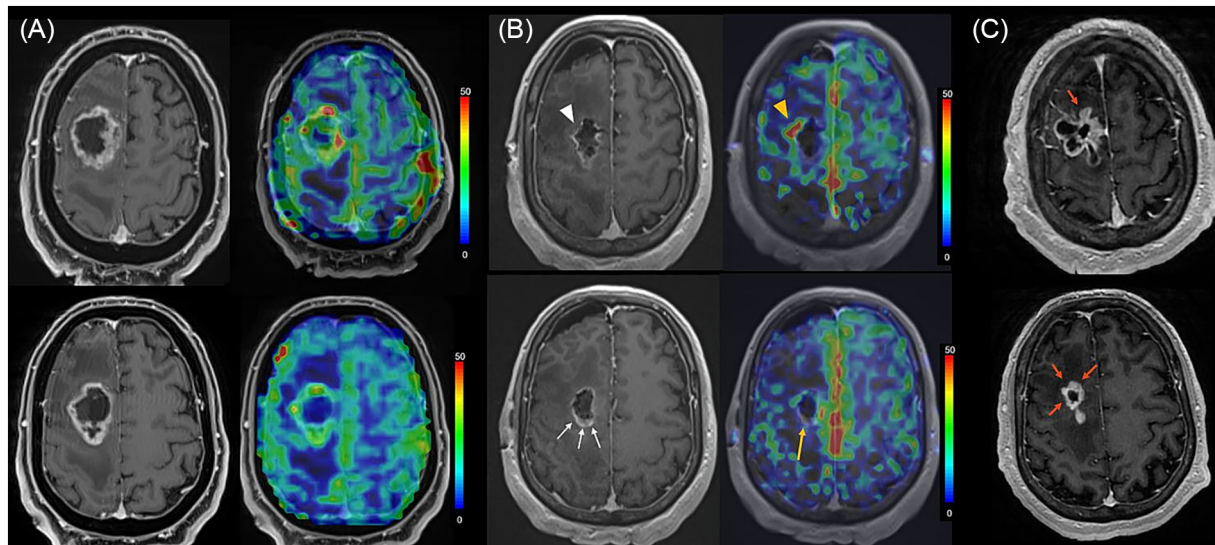


FIGURE 3 62-year-old male (No. 2 in Table 4). (A), Preoperative postcontrast T1w image and PCASL perfusion map overlaid on the postcontrast T_1 , showing a high-grade tumoral lesion with peripheral irregular nodular components surrounding necrosis (cytology confirmed a WHO Grade 4 glioblastoma, IDH 1 wildtype). (B), Intraoperative postcontrast T1w image and PCASL perfusion map overlaid on T_1 . On the superior slice PCASL evidenced a high-CBF area (yellow arrowhead) that did not present enhancing component on T_1 (white arrowhead) and did not correspond to a vascular structure, which was suggestive of residual tumor. On the inferior slice, the postcontrast T1w image showed a thickened contrast enhancing component within the posterior wall of the cavity that was recommended to review (white arrows). At this location the PCASL CBF map showed no hyperperfusion (yellow arrow). (C), Six-month follow-up postcontrast T1w image showing progression of the tumor in the cavity margins (red arrows). Two different slices are shown in the two rows.

PLD recommended for adult clinical patients in the brain ASL consensus paper²⁴ and a long LT, which effectively prolonged the delay time for the blood spins that were labeled earlier. Despite this, in these three patients the perfusion images displayed intravascular artifacts and low parenchymal perfusion, while one of the patients (70 years old) presented intravascular artifacts in the presurgery CBF maps as well. Nonetheless the neuroradiologists considered that these images had sufficient information to allow detection of residual tumor and found that, in two of the three patients, the CBF maps revealed possible hyperperfused residual component in the periphery of the surgical cavity (for details see Data S1 Section 1). This high perfusion signal could be due to abnormal blood vessels generated in the tumoral and peritumoral area, where neoangiogenic phenomena can occur.⁴⁴

Nevertheless, to reduce ATT artifacts there are more sophisticated models for CBF quantification, which can be applied to multiple PLD acquisitions. Multi-PLD ASL could be of interest in iMRI, as it enables the quantification of both CBF and ATT, providing additional information about the hemodynamics in each individual. However, as more parameters are introduced, more measurements and processing are needed, and this is an ongoing topic of research to be considered in future studies.

Consistent with the work of Lindner et al.,³¹ in this study PCASL proved to be a reliable tool to assess brain perfusion intraoperatively, arising as a complement to the anatomical sequences for the evaluation of residual tumor. In one patient of our cohort ASL depicted an additional area

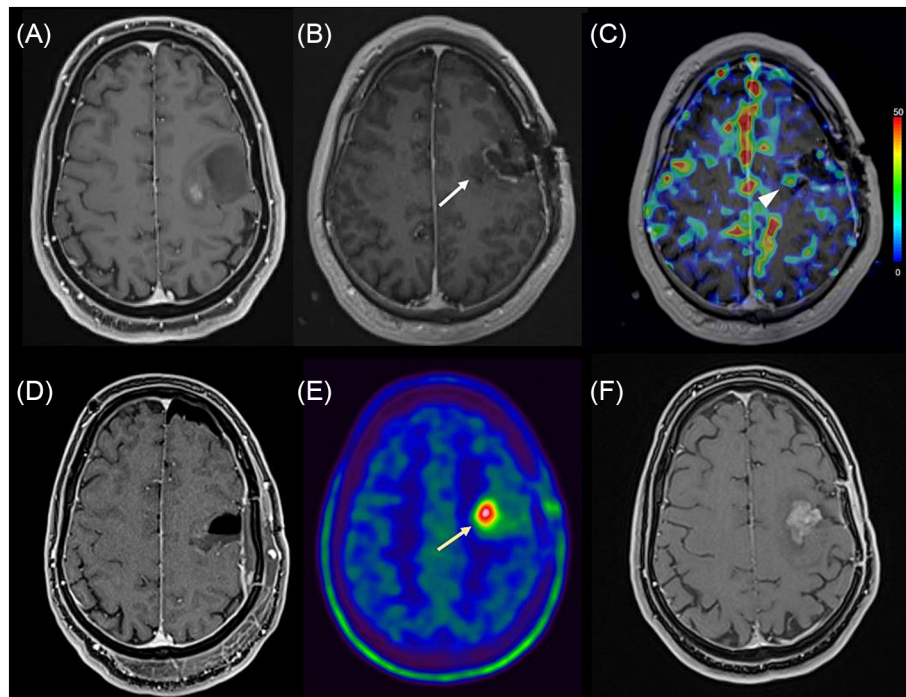


FIGURE 4 47-year-old patient (No. 1 in Table 4). (A), A preoperative postcontrast T1w image showed an expansive lesion in the left precentral gyrus with a small enhancing component, suggestive of anaplastic degeneration of a primary glial tumor (cytology confirmed a WHO Grade 3 astrocytoma). (B), An intraoperative postcontrast T1w image showed complete resection of the enhancing component with residual non-enhancing low-grade component in the medial aspect of the surgical cavity (white arrow). Neurosurgeons were aware that this component, also fluorescent with 5-ALA, was close to the corticospinal tract. Surgery continued and the residual component was resected up to 3 mm distance from the tract. (C), An intraoperative PCASL CBF map (overlaid on the postcontrast T1w image for anatomical reference) showed a spot of high CBF in the non-enhancing residual tumor (white arrowhead). (D), An early postoperative postcontrast T1w image revealed no enhancing residual components. (E), ¹¹C-methionine-PET performed one month postsurgery revealed increased metabolic activity in the medial border of the surgical cavity (yellow arrow). (F), Six-month follow-up postcontrast T1w image showing growth of the enhancing component, which together with other images suggested progression.

of high CBF that was not visible with the conventional sequences, as shown in Figure 3, and in two patients areas of hyperperfusion were found within non-enhancing residual tumor (Figure 4). These areas indicated neovascularization, known to be correlated with higher-grade component. Our findings highlight the additional value of this technique in the iMRI setting to achieve maximal safe resection of as much contrast enhancing component and hyperperfused tissue as possible. In the follow-up of those patients, these components grew rapidly, consistent with tumor progression.

Figure 5 demonstrates how in some highly vascularized tumors PCASL has the potential to better delineate residual tumor than conventional sequences. In this sense, in a tumor with scarce vascularization performing this sequence will probably not be of much use.

In the quantitative evaluation of CBF ratios, pre- and intraoperative PCASL values were comparable in the presumed residual tumor of the patients with incomplete resection. On the other hand, statistical differences were found in patients with gross total resection of the enhancing and hyperperfused components, as expected. In agreement with previous studies, CBF ratios in our sample matched the grades of gliomas determined by histopathology.^{28,43,45} The only patient with low-grade astrocytoma (No. 6) had an intraoperative CBF ratio of 1.09 (Table 4) (no preoperative PCASL data were available). In the patients with high-grade tumors preoperative values varied from 1.43 to 6.75. A previous study by Weber et al.⁴⁶ set a cut-off for CBF ratio greater than 1.6 to achieve high diagnostic performance in the differentiation between low- and high-grade gliomas (94% sensitivity, 78% specificity, 94% positive predictive value and 78% negative predictive value). In our study, two patients with glioblastoma Grade 4 (Nos. 8 and 9) had lower values of 1.43 and 1.51, respectively. Wolf et al.⁴⁷ referred also cases of patients whose measurements appeared to be different than expected. In their study they established the cut-off as 1.3 for the high-grade group. We only have one patient with metastasis, which can have variable CBF values (this patient presented a CBF ratio of 1.87).

In our cohort, interobserver agreement for image quality of PCASL CBF maps was substantial (Fleiss $\kappa = 0.76$). Agreement for the depiction of residual tumor with the PCASL sequences (Fleiss $\kappa = 0.80$) was only slightly lower than that of the evaluation of the conventional sequences (Fleiss $\kappa = 0.92$), which was almost perfect. Similar results were reported by Lindner et al.³¹ It must be noted that we evaluated the agreement among three readers, which is not very common and may slightly underestimate the results.

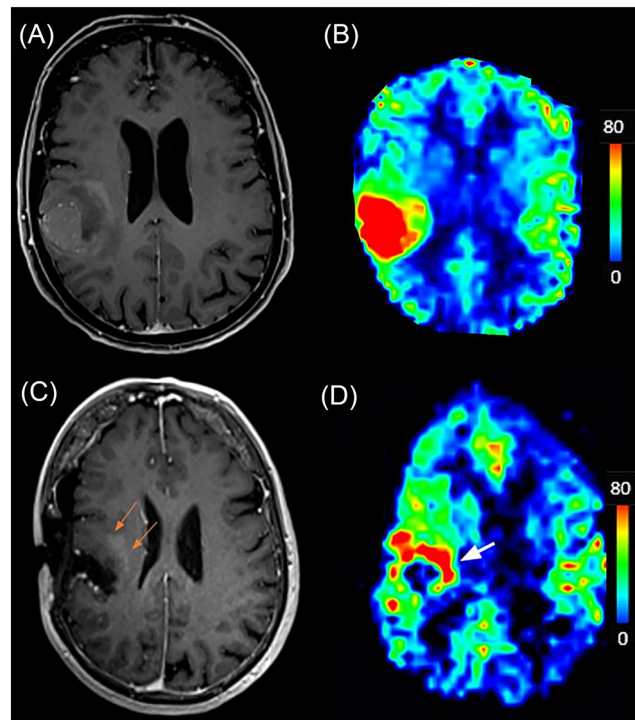


FIGURE 5 81-year-old patient (No. 10 in Table 4). (A), Preoperative postcontrast T1w image showing a right frontotemporal solid mass with faint enhancing component and no necrosis, suggestive of primary glial tumor (cytology confirmed a WHO Grade 3 oligodendroglioma). (B), A preoperative PCASL sequence showed very high CBF that appeared to extend outside the enhancing component, typical of glial tumors. (C), Intraoperative postcontrast T1w showed resection of the majority of the mass with residual faint enhancing component in the medial aspect of the surgical cavity (orange arrows). (D), An intraoperative PCASL map showed high CBF in the anterior and medial aspect of the surgical cavity, also extending beyond the enhancing lesion (white arrow). Neurosurgeons were aware of this component, but further resection could not be performed due to closeness to tract fibers.

Even though according to the purpose of this study the analysis was conducted at a second stage to assess the feasibility of this technique, it would be possible to carry out the visual analysis of CBF maps in real time to support the clinical decision-making.

4.1 | Limitations

One limitation of this study is that it has been performed in one center, and our results may not be extrapolated for general purposes. Also, the relatively small sample size could be viewed as a drawback, but it was limited by the number of brain tumor patients referred for surgery in our center. The order in which the images were scored can also be considered a limitation, because the PCASL images were first assessed to score image quality, and this could have influenced the subsequent scoring of residual tumor. This was minimized by defining strict criteria for scoring; nonetheless, the effect cannot be completely ruled out. Finally, tissue resected in the second resection was not separately evaluated histologically and could not be used to confirm residual tumor.

In conclusion, intraoperative PCASL is feasible at 3 T and shows potential for the assessment of residual tumor, providing additional information to the conventional sequences in some cases. Further work is warranted to provide conclusive evidence of its clinical utility by conducting a prospective clinical trial with a predefined gold standard for residual tumor (such as for example, targeted biopsy).

The CBF ratio, in addition to the qualitative information given by the contrast-enhanced T1w images, could be a useful tool in the evaluation of the histopathologic grade of the residual component, outlining components that could be beneficial to resect; however, further work is needed to investigate this point.

Furthermore intraoperative PCASL could also be of interest in patients where contrast media is contraindicated or in non-enhancing tumors, where contrast administration is not helpful in the evaluation of resection, providing additional information to T_2 -weighted images.

ORCID

Marta Calvo-Imirizaldu  <https://orcid.org/0000-0002-9063-401X>

María A. Fernández-Seara  <https://orcid.org/0000-0001-8536-6295>

REFERENCES

- Ohgaki H. Epidemiology of brain tumors. In: *Cancer Epidemiology (Methods in Molecular Biology Vol. 472)*. Humana; 2009:323-342. doi:10.1007/978-1-60327-492-0_14
- Louis DN, Perry A, Wesseling P, et al. The 2021 WHO Classification of Tumors of the Central Nervous System: a summary. *Neuro-Oncology*. 2021; 23(8):1231-1251. doi:10.1093/neuonc/noab106
- Nayak L, Lee EQ, Wen PY. Epidemiology of brain metastases. *Curr Oncol Rep*. 2012;14(1):48-54. doi:10.1007/s11912-011-0203-y
- Stupp R, Mason WP, van den Bent MJ, et al. Radiotherapy plus concomitant and adjuvant temozolomide for glioblastoma. *N Engl J Med*. 2005;352(10):987-996. doi:10.1056/NEJMoa043330
- Lacroix M, Abi-Said D, Fourney DR, et al. A multivariate analysis of 416 patients with glioblastoma multiforme: prognosis, extent of resection, and survival. *J Neurosurg*. 2001;95(2):190-198. doi:10.3171/jns.2001.95.2.0190
- Sanai N, Polley M-Y, McDermott MW, Parsa AT, Berger MS. An extent of resection threshold for newly diagnosed glioblastomas. *J Neurosurg*. 2011; 115(1):3-8. doi:10.3171/2011.2.JNS10998
- Oppenlander ME, Wolf AB, Snyder LA, et al. An extent of resection threshold for recurrent glioblastoma and its risk for neurological morbidity. *J Neurosurg*. 2014;120(4):846-853. doi:10.3171/2013.12.JNS13184
- Roelz R, Strohmaier D, Jabbarli R, et al. Residual tumor volume as best outcome predictor in low grade glioma—a nine-years near-randomized survey of surgery vs. biopsy. *Sci Rep*. 2016;6(1):32286. doi:10.1038/srep32286
- Aghi MK, Nahed BV, Sloan AE, Ryken TC, Kalkanis SN, Olson JJ. The role of surgery in the management of patients with diffuse low grade glioma: a systematic review and evidence-based clinical practice guideline. *J Neurooncol*. 2015;125(3):503-530. doi:10.1007/s11060-015-1867-1
- Hervey-Jumper SL, Berger MS. Maximizing safe resection of low- and high-grade glioma. *J Neurooncol*. 2016;130(2):269-282. doi:10.1007/s11060-016-2110-4
- Hatiboglu MA, Weinberg JS, Suki D, et al. Impact of intraoperative high-field magnetic resonance imaging guidance on glioma surgery. *Neurosurgery*. 2009;64(6):1073-1081. doi:10.1227/01.NEU.0000345647.58219.07
- Smets T, Lawson TM, Grandin C, Jankovski A, Raftopoulos C. Immediate post-operative MRI suggestive of the site and timing of glioblastoma recurrence after gross total resection: a retrospective longitudinal preliminary study. *Eur Radiol*. 2013;23(6):1467-1477. doi:10.1007/s00330-012-2762-1
- Garcia-Ruiz A, Naval-Baudin P, Ligerio M, et al. Precise enhancement quantification in post-operative MRI as an indicator of residual tumor impact is associated with survival in patients with glioblastoma. *Sci Rep*. 2021;11(1):695. doi:10.1038/s41598-020-79829-3
- Kotrotsou A, Elakkad A, Sun J, et al. Multi-center study finds postoperative residual non-enhancing component of glioblastoma as a new determinant of patient outcome. *J Neurooncol*. 2018;139(1):125-133. doi:10.1007/s11060-018-2850-4
- Masuda Y, Akutsu H, Ishikawa E, et al. Evaluation of the extent of resection and detection of ischemic lesions with intraoperative MRI in glioma surgery: is intraoperative MRI superior to early postoperative MRI? *J Neurosurg*. 2019;131(1):209-216. doi:10.3171/2018.3.JNS172516
- Senft C, Seifert V, Hermann E, Franz K, Gasser T. Usefulness of intraoperative ultra low-field magnetic resonance imaging in glioma surgery. *Oper Neurosurg*. 2008;63(Suppl 4):ONS257-ONS267. doi:10.1227/01.NEU.0000313624.77452.3C
- Pino M, Imperato A, Musca I, et al. New hope in brain glioma surgery: the role of intraoperative ultrasound. A review. *Brain Sci*. 2018;8(11):202. doi:10.3390/brainsci8110202
- Belsuzarri TB, Sangenis RA, Araujo JM. Brain tumor surgery: supplemental intra-operative imaging techniques and future challenges. *J Cancer Metastasis Treat*. 2015;2(0):70-79. doi:10.4103/2394-4722.172249
- Senft C, Bink A, Franz K, Vatter H, Gasser T, Seifert V. Intraoperative MRI guidance and extent of resection in glioma surgery: a randomised, controlled trial. *Lancet Oncol*. 2011;12(11):997-1003. doi:10.1016/S1470-2045(11)70196-6
- Krivosheya D, Prabhu SS. Combining functional studies with intraoperative MRI in glioma surgery. *Neurosurg Clin N Am*. 2017;28(4):487-497. doi:10.1016/j.nec.2017.05.004
- Rogers CM, Jones PS, Weinberg JS. Intraoperative MRI for brain tumors. *J Neurooncol*. 2021;151(3):479-490. doi:10.1007/s11060-020-03667-6
- Ulmer S, Helle M, Jansen O, Mehdorn HM, Nabavi A. Intraoperative dynamic susceptibility contrast weighted magnetic resonance imaging (iDSC-MRI)—technical considerations and feasibility. *NeuroImage*. 2009;45(1):38-43. doi:10.1016/j.neuroimage.2008.11.021
- Ulmer S, Hartwigens G, Riedel C, Jansen O, Mehdorn HM, Nabavi A. Intraoperative dynamic susceptibility contrast MRI (iDSC-MRI) is as reliable as preoperatively acquired perfusion mapping. *NeuroImage*. 2010;49(3):2158-2162. doi:10.1016/j.neuroimage.2009.10.084
- Alsop DC, Detre JA, Golay X, et al. Recommended implementation of arterial spin-labeled perfusion MRI for clinical applications: a consensus of the ISMRM Perfusion Study Group and the European Consortium for ASL in Dementia. *Magn Reson Med*. 2015;73(1):102-116. doi:10.1002/mrm.25197
- Järnum H, Steffensen EG, Knutsson L, et al. Perfusion MRI of brain tumours: a comparative study of pseudo-continuous arterial spin labelling and dynamic susceptibility contrast imaging. *Neuroradiology*. 2010;52(4):307-317. doi:10.1007/s00234-009-0616-6
- Cebeci H, Aydin O, Ozturk-Isik E, et al. Assessment of perfusion in glial tumors with arterial spin labeling; comparison with dynamic susceptibility contrast method. *Eur J Radiol*. 2014;83(10):1914-1919. doi:10.1016/j.ejrad.2014.07.002
- Lehmann P, Monet P, de Marco G, et al. A comparative study of perfusion measurement in brain tumours at 3 Tesla MR: arterial spin labeling versus dynamic susceptibility contrast-enhanced MRI. *Eur Neurol*. 2010;64(1):21-26. doi:10.1159/000311520
- Jezzard P, Chappell MA, Okell TW. Arterial spin labeling for the measurement of cerebral perfusion and angiography. *J Cereb Blood Flow Metab*. 2018; 38(4):603-626. doi:10.1177/0271678X17743240
- ElBeheiry AA, Emara DM, Abdel-Latif AAB, Abbas M, Ismail AS. Arterial spin labeling in the grading of brain gliomas: could it help? *Egypt J Radiol Nucl Med*. 2020;51(1):235. doi:10.1186/s43055-020-00352-6
- Lindner T, Ahmeti H, Lübging I, et al. Intraoperative resection control using arterial spin labeling—proof of concept, reproducibility of data and initial results. *NeuroImage Clin*. 2017;15(February):136-142. doi:10.1016/j.nicl.2017.04.021
- Lindner T, Ahmeti H, Juhasz J, et al. A comparison of arterial spin labeling and dynamic susceptibility perfusion imaging for resection control in glioblastoma surgery. *Oncotarget*. 2018;9(26):18570-18577. doi:10.18632/oncotarget.24970
- Venkatraghavan L, Manninen P, Mak P, Lukitto K, Hodaie M, Lozano A. Anesthesia for functional neurosurgery. *J Neurosurg Anesthesiol*. 2006;18(1):64-67. doi:10.1097/01.ana.0000181285.71597.e8
- Rasmussen M, Juul N, Christensen SM, et al. Cerebral blood flow, blood volume, and mean transit time responses to propofol and indomethacin in peritumor and contralateral brain regions. *Anesthesiology*. 2010;112(1):50-56. doi:10.1097/ALN.0b013e3181c38bd3

34. Conti A, Iacopino DG, Fodale V, Micalizzi S, Penna O, Santamaria LB. Cerebral haemodynamic changes during propofol–remifentanyl or sevoflurane anaesthesia: transcranial Doppler study under bispectral index monitoring. *Br J Anaesth*. 2006;97(3):333–339. doi:10.1093/bja/ael169
35. Vidorreta M, Balteau E, Wang Z, et al. Evaluation of segmented 3D acquisition schemes for whole-brain high-resolution arterial spin labeling at 3 T. *NMR Biomed*. 2014;27(11):1387–1396. doi:10.1002/nbm.3201
36. Buxton RB, Frank LR, Wong EC, Siewert B, Warach S, Edelman RR. A general kinetic model for quantitative perfusion imaging with arterial spin labeling. *Magn Reson Med*. 1998;40(3):383–396. doi:10.1002/mrm.1910400308
37. Ferro DA, Mutsaerts HJJM, Hilal S, et al. Cortical microinfarcts in memory clinic patients are associated with reduced cerebral perfusion. *J Cereb Blood Flow Metab*. 2020;40(9):1869–1878. doi:10.1177/0271678X19877403
38. Knopp EA, Cha S, Johnson G, et al. Glial neoplasms: dynamic contrast-enhanced T_2^* -weighted MR imaging. *Radiology*. 1999;211(3):791–798. doi:10.1148/radiology.211.3.r99jn46791
39. Shin JH, Lee HK, Kwun BD, et al. Using relative cerebral blood flow and volume to evaluate the histopathologic grade of cerebral gliomas: preliminary results. *Am J Roentgenol*. 2002;179(3):783–789. doi:10.2214/ajr.179.3.1790783
40. Landis JR, Koch GG. The measurement of observer agreement for categorical data. *Biometrics*. 1977;33(1):159–174. doi:10.2307/2529310
41. Fan AP, Guo J, Khalighi MM, et al. Long-delay arterial spin labeling provides more accurate cerebral blood flow measurements in Moyamoya patients a simultaneous positron emission tomography/MRI study. *Stroke*. 2017;48(9):2441–2449. doi:10.1161/STROKEAHA.117.017773
42. Amukotuwa SA, Yu C, Zaharchuk G. 3D pseudocontinuous arterial spin labeling in routine clinical practice: a review of clinically significant artifacts. *J Magn Reson Imaging*. 2016;43(1):11–27. doi:10.1002/jmri.24873
43. Kim MJ, Kim HS, Kim J-H, Cho K-G, Kim SY. Diagnostic accuracy and interobserver variability of pulsed arterial spin labeling for glioma grading. *Acta Radiol*. 2008;49(4):450–457. doi:10.1080/02841850701881820
44. Ahir BK, Engelhard HH, Lakka SS. Tumor development and angiogenesis in adult brain tumor: glioblastoma. *Mol Neurobiol*. 2020;57(5):2461–2478. doi:10.1007/s12035-020-01892-8
45. Falk Delgado A, De Luca F, van Westen D, Falk DA. Arterial spin labeling MR imaging for differentiation between high- and low-grade glioma—a meta-analysis. *Neuro-Oncology*. 2018;20(11):1450–1461. doi:10.1093/neuonc/nyy095
46. Weber MA, Zoubaa S, Schlieter M, et al. Diagnostic performance of spectroscopic and perfusion MRI for distinction of brain tumors. *Neurology*. 2006;66(12):1899–1906. doi:10.1212/01.wnl.0000219767.49705.9c
47. Wolf RL, Wang J, Wang S, et al. Grading of CNS neoplasms using continuous arterial spin labeled perfusion MR imaging at 3 Tesla. *J Magn Reson Imaging*. 2005;22(4):475–482. doi:10.1002/jmri.20415

SUPPORTING INFORMATION

Additional supporting information can be found online in the Supporting Information section at the end of this article.

How to cite this article: Calvo-Imirizaldu M, Aramendía-Vidaurreta V, Sánchez-Albardíaz C, et al. Clinical utility of intraoperative arterial spin labeling for resection control in brain tumor surgery at 3 T. *NMR in Biomedicine*. 2023;36(9):e4938. doi:10.1002/nbm.4938